Electronic Supplementary Material (ESI) for Physical Chemistry Chemical Physics.

Supporting Material:

O-H vibrational motions promote sub-50 fs nonadiabatic dynamics in 3-hydroxypyran-4-one : Interplay between internal conversion and ESIPT

Neethu Anand,[†] Probal Nag,[†] Ravi Kumar Kanaparthi,[*,‡] and Sivaranjana Reddy Vennapusa[*,†]

†*Indian Institute of Science Education and Research Thiruvananthapuram, Maruthamala PO, Vithura, Thiruvananthapuram 695551, India*

‡*Central University of Kerala, School of Physical Sciences, Tejaswini Hills, Periya, Kerala 671320, India*

E-mail: rkchem@cukerala.ac.in; siva@iisertvm.ac.in

Table of contents

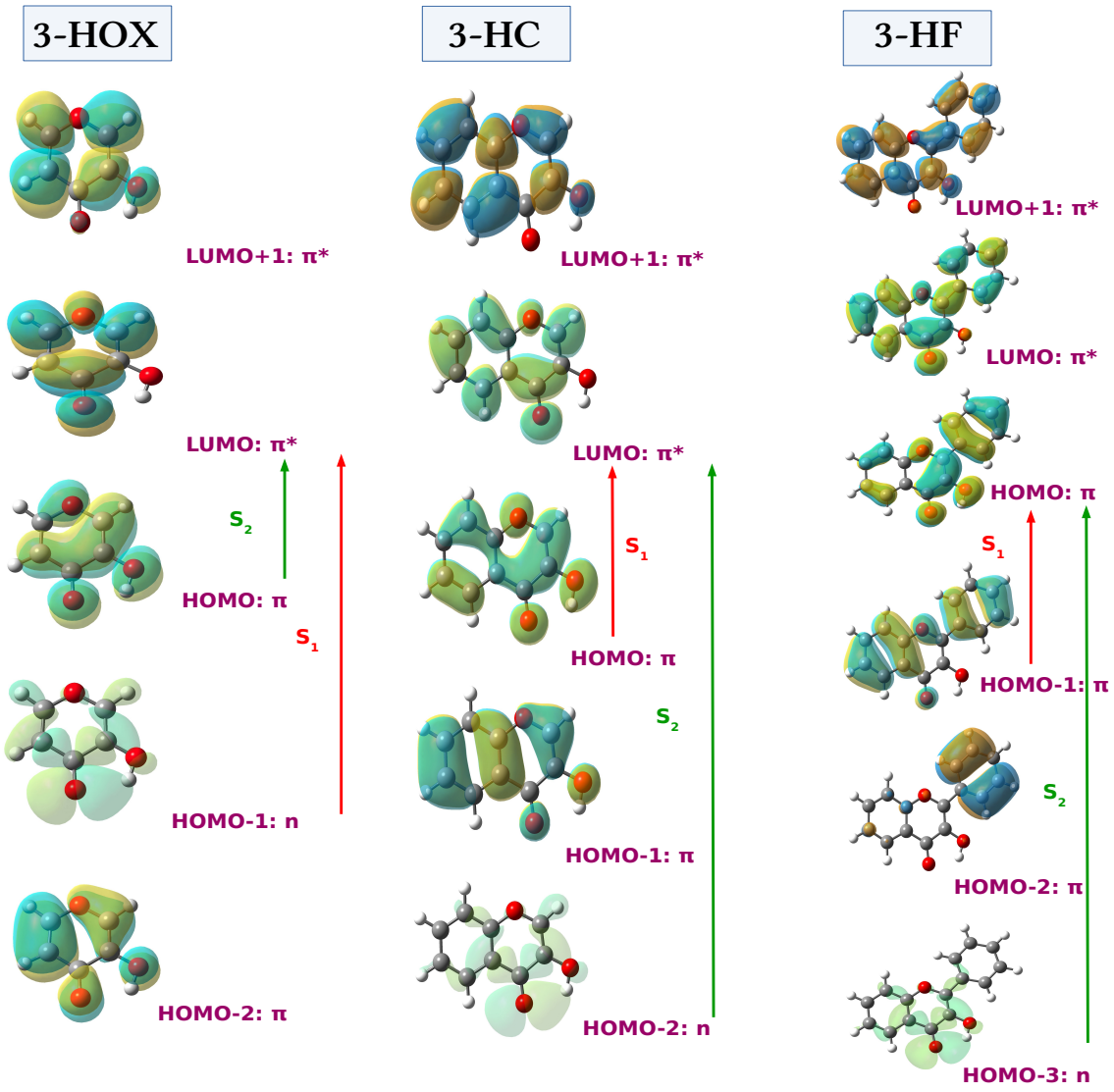

SM1: Frontier molecular orbitals of 3HOX (3-hydroxy-2-pyrone), 3HC (3-hydroxychromone) and 3HF (3-hydroxyflavone) obtained at B3LYP/6-311++G** level of theory. The vertical transition oscillator strength, f, of S_1 and S_2 states are given in parenthesis.

Table SM2: Numbering, symmetry and harmonic frequency components of vibrational modes of 3HOX calculated at B3LYP and CAM-B3LYP with the 6-311++G(d,p) level of theory.

	B3LYP	CAM-B3LYP
No.(Sym.)	ω(in cm^{-1})	ω(in cm^{-1})
$\nu_1(a'')$	156.1187	155.2476
$\nu_2(a'')$	294.8692	300.8056
$\nu_3(a')$	304.4567	309.1258
$\nu_4(a'')$	405.2689	408.4052
$\nu_5(a')$	459.3979	463.9359
$\nu_6(a'')$	522.5628	527.4913
$\nu_7(a')$	564.0986	571.4880
$\nu_8(a')$	598.0276	605.6345
$\nu_9(a'')$	615.6084	606.6996
$\nu_{10}(a'')$	742.7613	752.0911
$\nu_{11}(a')$	762.7264	776.0833
$\nu_{12}(a'')$	827.8404	841.8632
$\nu_{13}(a'')$	845.1885	868.3543
$\nu_{14}(a')$	883.4481	895.7784
$\nu_{15}(a'')$	947.2509	976.4400
$\nu_{16}(a')$	1005.1597	1024.8686
$\nu_{17}(a')$	1119.4547	1140.6116
$\nu_{18}(a')$	1209.0360	1220.6587
$\nu_{19}(a')$	1277.7829	1292.4934
$\nu_{20}(a')$	1281.4350	1301.7508
$\nu_{21}(a')$	1341.9677	1358.6890
$\nu_{22}(a')$	1427.8683	1443.4241
$\nu_{23}(a')$	1468.0179	1502.1466
$\nu_{24}(a')$	1608.7256	1650.3827
$\nu_{25}(a')$	1687.1427	1734.5041
$\nu_{26}(a')$	1694.6784	1742.2511
$\nu_{27}(a')$	3206.8844	3231.4065
$\nu_{28}(a')$	3226.7817	3248.9761
$\nu_{29}(a')$	3243.9458	3265.5342
$\nu_{30}(a')$	3608.9645	3661.8998

Table SM3: Linear intrastate coupling parameters (κ) of S_1 and S_2 states of 3HOX using TD-B3LYP/6-311++G** and TD-CAMB3LYP/6-311++G** level of theory. All values are in eV. The coupling strength ($\kappa^2/2\omega^2$) is given in the paranthesis.

	TD-B3LYP			TD-CAMB3LYP	
a' mode [frequency]	κ^{S_1}	κ^{S_2}	a' mode	κ^{S_1}	κ^{S_2}
ν_3 [0.0377]	-0.0635 (1.42)	0.0396 (0.55)	ν_3 [0.0383]	-0.0663 (1.50)	0.0401 (0.55)
ν_5 [0.0570]	-0.0057 (0.00)	-0.0762 (0.89)	ν_5 [0.0575]	-0.0029 (0.00)	-0.0782 (0.92)
ν_7 [0.0699]	-0.0134 (0.02)	-0.0092 (0.01)	ν_7 [0.0709]	-0.0097 (0.01)	-0.0101 (0.01)
ν_8 [0.0741]	0.0310 (0.09)	-0.0354 (0.11)	ν_8 [0.0751]	0.0321 (0.09)	-0.0370 (0.12)
ν_{11} [0.0946]	-0.0041 (0.00)	0.0702 (0.28)	ν_{11} [0.0962]	0.0141 (0.01)	0.0540 (0.16)
ν_{14} [0.1095]	-0.0336 (0.05)	0.0221 (0.02)	ν_{14} [0.1111]	-0.0262 (0.03)	0.0526 (0.11)
ν_{16} [0.1246]	0.0768 (0.19)	0.1257 (0.51)	ν_{16} [0.1271]	0.0676 (0.14)	0.1217 (0.46)
ν_{17} [0.1388]	-0.0373 (0.04)	0.0153 (0.01)	ν_{17} [0.1414]	-0.0343 (0.03)	0.0143 (0.01)
ν_{18} [0.1499]	-0.0389 (0.03)	-0.0312 (0.02)	ν_{18} [0.1513]	-0.0170 (0.01)	-0.0097 (0.00)
ν_{19} [0.1584]	0.0422 (0.04)	0.0543 (0.06)	ν_{19} [0.1602]	0.0452 (0.04)	-0.0119 (0.00)
ν_{20} [0.1589]	0.0494 (0.05)	-0.0338 (0.02)	ν_{20} [0.1614]	0.0359 (0.02)	0.0390 (0.03)
ν_{21} [0.1664]	0.0090 (0.00)	-0.1207 (0.26)	ν_{21} [0.1685]	0.0080 (0.00)	-0.1108 (0.22)
ν_{22} [0.1770]	-0.0428 (0.03)	0.0896 (0.13)	ν_{22} [0.1790]	-0.0557 (0.05)	0.0686 (0.07)
ν_{23} [0.1820]	0.0042 (0.00)	0.1157 (0.20)	ν_{23} [0.1862]	-0.0077 (0.00)	0.1104 (0.18)
ν_{24} [0.1995]	0.0699 (0.06)	0.0570 (0.04)	ν_{24} [0.2046]	0.0747 (0.07)	0.0933 (0.10)
ν_{25} [0.2092]	0.2690 (0.83)	0.1106 (0.14)	ν_{25} [0.2151]	0.1721 (0.32)	0.1672 (0.30)
ν_{26} [0.2101]	0.1023 (0.12)	-0.0622 (0.04)	ν_{26} [0.2160]	0.1926 (0.40)	-0.0419 (0.02)
ν_{27} [0.3976]	0.0053 (0.00)	0.0109 (0.00)	ν_{27} [0.4006]	0.0029 (0.00)	0.0160 (0.00)
ν_{28} [0.4001]	-0.0109 (0.00)	-0.0255 (0.00)	ν_{28} [0.4028]	-0.0062 (0.00)	-0.0187 (0.00)
ν_{29} [0.4022]	-0.0081 (0.00)	-0.0080 (0.00)	ν_{29} [0.4049]	-0.0058 (0.00)	-0.0135 (0.00)
ν_{30} [0.4475]	-0.0698 (0.01)	0.0689 (0.01)	ν_{30} [0.4540]	-0.0659 (0.01)	0.0675 (0.01)

Table SM4: Linear intrastate coupling parameters (κ) of S_1 and S_2 states of 3HOX using EOM-CCSD/6-311++G** and RI-CC2/6-311++G** level of theory. All values are in eV. The coupling strength ($\kappa^2/2\omega^2$) is given in the paranthesis.

	EOM-CCSD			RI-CC2	
a' mode [frequency]	κ^{S_1}	κ^{S_2}	a' mode	κ^{S_1}	κ^{S_2}
ν_3 [0.0377]	-0.0585 (1.21)	0.0479 (0.81)	ν_3 [0.0377]	-0.0487 (0.83)	0.0509 (0.91)
ν_5 [0.0570]	-0.0022 (0.00)	-0.0707 (0.77)	ν_5 [0.0570]	-0.0059 (0.01)	-0.0743 (0.85)
ν_7 [0.0699]	-0.0094 (0.01)	0.0033 (0.00)	ν_7 [0.0699]	-0.0124 (0.02)	0.0042 (0.00)
ν_8 [0.0741]	0.0329 (0.10)	-0.0327 (0.10)	ν_8 [0.0741]	0.0308 (0.09)	-0.0373 (0.13)
ν_{11} [0.0946]	0.0148 (0.01)	0.0428 (0.10)	ν_{11} [0.0946]	-0.0085 (0.00)	0.0654 (0.24)
ν_{14} [0.1095]	-0.0212 (0.02)	0.0933 (0.36)	ν_{14} [0.1095]	-0.0229 (0.02)	0.0726 (0.22)
ν_{16} [0.1246]	0.0686 (0.15)	0.1217 (0.48)	ν_{16} [0.1246]	0.0717 (0.17)	0.1309 (0.55)
ν_{17} [0.1388]	-0.0265 (0.02)	0.0299 (0.02)	ν_{17} [0.1388]	-0.0285 (0.02)	0.0258 (0.02)
ν_{18} [0.1499]	-0.0167 (0.01)	-0.0417 (0.05)	ν_{18} [0.1499]	-0.0422 (0.04)	-0.0279 (0.02)
ν_{19} [0.1584]	0.0291 (0.02)	0.0491 (0.05)	ν_{19} [0.1584]	0.0402 (0.03)	0.0581 (0.07)
ν_{20} [0.1589]	0.0432 (0.04)	-0.0222 (0.01)	ν_{20} [0.1589]	0.0441 (0.04)	-0.0386 (0.03)
ν_{21} [0.1664]	0.0101 (0.00)	-0.1270 (0.29)	ν_{21} [0.1664]	0.0106 (0.00)	-0.1420 (0.36)
ν_{22} [0.1770]	-0.0646 (0.07)	0.0846 (0.11)	ν_{22} [0.1770]	-0.0538 (0.05)	0.0906 (0.13)
ν_{23} [0.1820]	-0.0074 (0.00)	0.1166 (0.21)	ν_{23} [0.1820]	-0.0089 (0.00)	0.1260 (0.24)
ν_{24} [0.1995]	0.0960 (0.12)	0.0728 (0.07)	ν_{24} [0.1995]	0.0873 (0.10)	0.0914 (0.10)
ν_{25} [0.2092]	0.2728 (0.85)	0.1990 (0.45)	ν_{25} [0.2092]	0.3390 (1.31)	0.1488 (0.25)
ν_{26} [0.2101]	0.1230 (0.17)	-0.1098 (0.13)	ν_{26} [0.2101]	0.1121 (0.14)	-0.0826 (0.08)
ν_{27} [0.3976]	0.0029 (0.00)	0.0176 (0.00)	ν_{27} [0.3976]	0.0059 (0.00)	0.0170 (0.00)
ν_{28} [0.4001]	-0.0055 (0.00)	-0.0269 (0.00)	ν_{28} [0.4001]	-0.0067 (0.00)	-0.0217 (0.00)
ν_{29} [0.4022]	-0.0051 (0.00)	-0.0141 (0.00)	ν_{29} [0.4022]	-0.0084 (0.00)	-0.0089 (0.00)
ν_{30} [0.4475]	-0.0580 (0.01)	0.0688 (0.01)	ν_{30} [0.4475]	-0.0610 (0.01)	0.0911 (0.02)

Table SM5: Linear interstate coupling parameters (λ) associated with S_1-S_2 states of 3HOX using TD-B3LYP/6-311++G** and TD-CAMB3LYP/6-311++G** level of theory. All values are in eV.

TD-B3LYP		TD-CAMB3LYP	
a" modes (Frequency)	$\lambda_{S_1-S_2}$	a" modes (Frequency)	$\lambda_{S_1-S_2}$
ν_1 (0.0194)	-	ν_1 (0.0192)	-
ν_2 (0.0366)	0.0296	ν_2 (0.0373)	0.0206
ν_4 (0.0502)	-	ν_4 (0.0506)	-
ν_6 (0.0648)	-	ν_6 (0.0654)	-
ν_9 (0.0763)	0.0648	ν_9 (0.0752)	0.0768
ν_{10} (0.0921)	0.0248	ν_{10} (0.0932)	0.0278
ν_{12} (0.1026)	0.0372	ν_{12} (0.1044)	0.0221
ν_{13} (0.1048)	0.0585	ν_{13} (0.1077)	0.0515
ν_{15} (0.1174)	-	ν_{15} (0.1211)	-

Table SM6: Linear interstate coupling parameters (λ) associated with S_1-S_2 states of 3HOX using EOM-CCSD/6-311++G** and RI-CC2/6-311++G** level of theory. All values are in eV.

EOM-CCSD		RI-CC2	
a" modes (Frequency)	$\lambda_{S_1-S_2}$	a" modes (Frequency)	$\lambda_{S_1-S_2}$
ν_1 (0.0194)	-	ν_1 (0.0194)	-
ν_2 (0.0366)	0.0232	ν_2 (0.0366)	0.0362
ν_4 (0.0502)	0.0201	ν_4 (0.0502)	0.0245
ν_6 (0.0648)	-	ν_6 (0.0648)	-
ν_9 (0.0763)	0.0924	ν_9 (0.0763)	0.0759
ν_{10}(0.0921)	-	ν_{10} (0.0921)	0.0133
ν_{12}(0.1026)	0.0270	ν_{12} (0.1026)	0.0381
ν_{13}(0.1048)	0.0412	ν_{13} (0.1048)	0.0564
ν_{15}(0.1174)	-	ν_{15} (0.1174)	-

MCTDH initial wavepacket

We have chosen a total 26 vibrational modes (out of 30, four non-totally symmetric modes i.e., a$''$, show zero inter-state coupling) based on their respective excitation strength (cf., SI3-SI6) for the wavepacket propagation calculations. The initial wavepacket ($\Psi_{\mathrm{f}}(0)$) is placed vertically on to the "bright" S_2 state, i.e., $\Psi_{\mathrm{f}}\,(\mathrm{t}) = \mathrm{e}^{-iHt/\hbar}\,\Psi_{\mathrm{f}}(0)$ where H is the 2x2 vibronic Hamiltonian. The wavepacket is then allowed to evolve for a period of 300 fs. The absorption spectrum is generated by Fourier transformation of the autocorrelation function of the wavepacket evolving on S_2 state. The intensity $I(E)$ of the spectrum is expressed as

$$I(E) \propto \int e^{iEt}\; a_(t)\; dt, \tag{1}$$

where $a(t)$ denotes the time autocorrelation function. The latter quantity is evaluated as $a(t) = \langle \Psi_f(0) | \Psi_f(t) \rangle$.

Number of basis functions for the primitive as well as the single-particle basis used in the MCTDH calculations are given in SM7-SM8.

Table SM7: MCTDH details of normal mode combination, size of the primitive and single particle bases used in the S_1-S_2 vibronic dynamics of 3HOX for TD-B3LYP and TD-CAMB3LYP vibronic coupling parameters.

	Normal modes	Primitive basis	SPF basis [S_1, S_2]
TD-B3LYP	(ν_3, ν_5, ν_7, ν_8, ν_{27}, ν_{28})	(9, 10, 6, 7, 4, 4)	[12, 14]
	(ν_{11}, ν_{14}, ν_{20}, ν_{29}, ν_{30})	(7, 6, 6, 4, 5)	[14,12]
	(ν_{16}, ν_{17}, ν_{18}, ν_2, ν_9)	(9, 6, 6, 10, 10)	[12, 14]
	(ν_{19}, ν_{21}, ν_{22}, ν_{10}, ν_{12})	(6, 7, 7, 4,6)	[12, 14]
	(ν_{23}, ν_{24}, ν_{25}, ν_{26}, ν_{13})	(7, 6, 10, 7, 7)	[14, 12]

	Normal modes	Primitive basis	SPF basis [S_1, S_2]
TD-CAMB3LYP	(ν_3, ν_5, ν_7, ν_8, ν_{27}, ν_{28})	(10, 9, 5, 6, 4, 4)	[12, 14]
	(ν_{11}, ν_{14}, ν_{20}, ν_{29}, ν_{30})	(6, 6, 5, 4, 5)	[14, 12]
	(ν_{16}, ν_{17}, ν_{18}, ν_2, ν_9)	(7, 5, 4, 7, 10)	[12, 14]
	(ν_{19}, ν_{21}, ν_{22}, ν_{10}, ν_{12})	(5, 6, 6, 5, 4)	[12, 14]
	(ν_{23}, ν_{24}, ν_{25}, ν_{26}, ν_{13})	(6, 6, 7, 7, 6)	[14, 12]

Table SM8: MCTDH details of normal mode combination, size of the primitive and single particle bases used in the S_1-S_2 vibronic dynamics of 3HOX for EOM-CCSD and RI-CC2 vibronic coupling parameters.

	Normal modes	Primitive basis	SPF basis [S_1, S_2]
EOM-CCSD	(ν_3, ν_5, ν_7, ν_8, ν_{27}, ν_{28})	(10, 7, 5, 7, 4, 4)	[12, 14]
	(ν_{11}, ν_{14}, ν_{20}, ν_{29}, ν_{30})	(6, 8, 5, 4, 4)	[14,12]
	(ν_{16}, ν_{17}, ν_{18}, ν_2, ν_4)	(8, 5, 5, 7, 6)	[12, 14]
	(ν_{19}, ν_{21}, ν_{22}, ν_9, ν_{12})	(5, 7, 6, 10, 5)	[12, 14]
	(ν_{23}, ν_{24}, ν_{25}, ν_{26}, ν_{13})	(7, 6, 9, 6, 6)	[14, 12]

	Normal modes	Primitive basis	SPF basis [S_1, S_2]
RI-CC2	(ν_3, ν_5, ν_7, ν_8, ν_{27}, ν_{28})	(9, 10, 6, 7, 4, 4)	[12, 14]
	(ν_{11}, ν_{14}, ν_{20}, ν_{29}, ν_{30})	(7, 6, 6, 4, 5)	[14, 12]
	(ν_{16}, ν_{17}, ν_{18}, ν_2, ν_9)	(9, 6, 6, 10, 10)	[12, 14]
	(ν_{19}, ν_{21}, ν_{22}, ν_{10}, ν_{12})	(6, 7, 7, 4, 6)	[12, 14]
	(ν_{23}, ν_{24}, ν_{25}, ν_{26}, ν_{13})	(7, 6, 10, 7, 7)	[14, 12]

In general, the primitive basis (time-independent) are chosen as discrete variable representation (DVR) such a harmonic oscillator functions, sine functions, Legendre functions etc. Here we chose harmonic oscillator DVR in the dimensionless coordinate system for the relevant vibrational mode. The primitive basis for each particle is the product of the one-dimensional bases; e.g for particle 1 in the set of TD-B3LYP (SM7), the primitive basis contains $9\times10\times6\times7\times4\times4= 60480$ functions and the full primitive basis consists of a total of 1.43×10^{21} functions. Similarly, a full primitive basis of 1.23×10^{20}, 1.81×10^{20} and 1.43×10^{21} for TD-CAMB3LYP, EOM-CCSD and RI-CC2 is employed, respectively.

The wavefunction expansion length is the total single-particle functions basis size. This quantity is equal to the product of the number of SPFs per particle, summed over the 2 states.

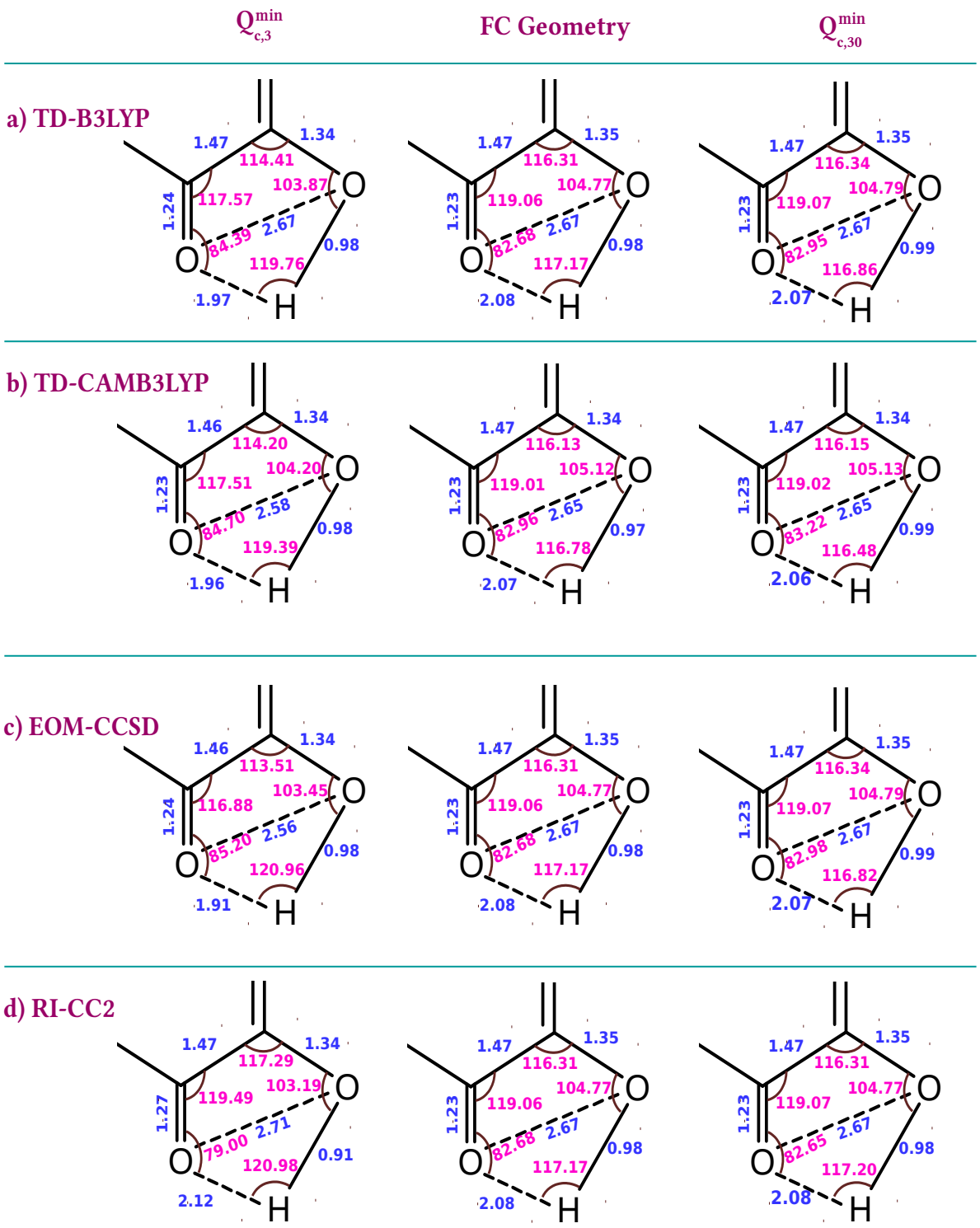

SM9: Structural parameters (distances in blue color and angles in magenta color) of the FC geometry, $Q^{min}_{c,3}$ and $Q^{min}_{c,30}$ of 3-HOX.

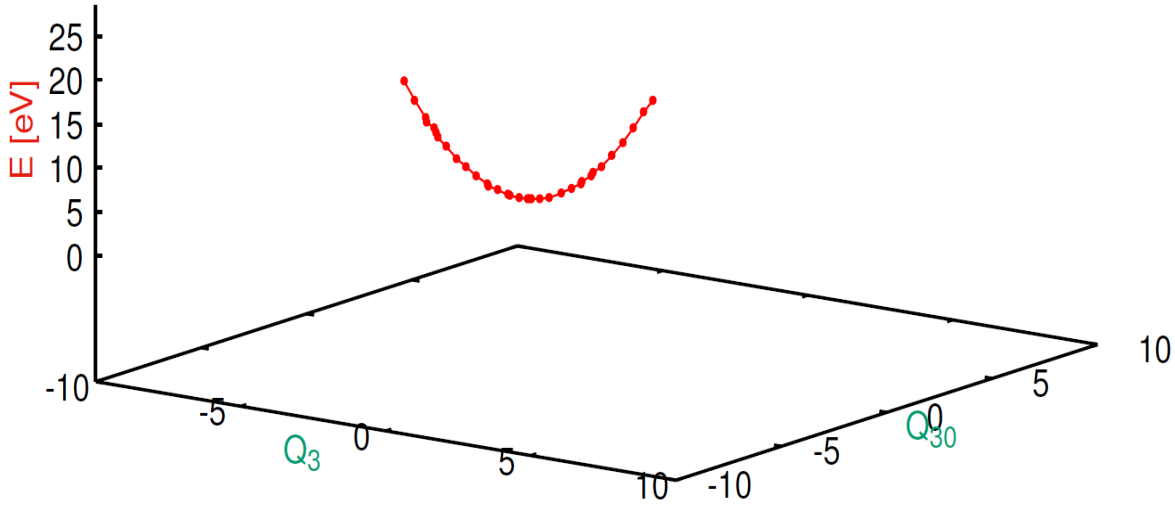

SM10: S_1-S_2 conical intersection seam between Q_3 and Q_{30} normal coordinate space of 3-HOX.

SM11: Experimental UV/vis spectroscopy measurements

3-HOX, procured from R Scientific (India), was recrystallized from ethanol and subsequently used in all photophysical studies. Solvents used in this study have been procured from Merck (India) and dried using appropriate drying agents and then distilled prior to spectral measurements. Optical absorption spectra were recorded on a Shimadzu (Model UV-3600) spectrophotometer. Concentrations of solutions are ca. to be 1.0 x 10^{-6} M.

We show experimental absorption spectral features of 3-HOX in Fig. 1 Two distinct absorption bands, centered at 4.7 eV and 5.9 eV, are observed. The intensity of lower energy band is found to be slightly smaller than the higher energy band (cf., Fig. 1). Both bands exhibit a broad structureless feature regardless of solvent polarity.

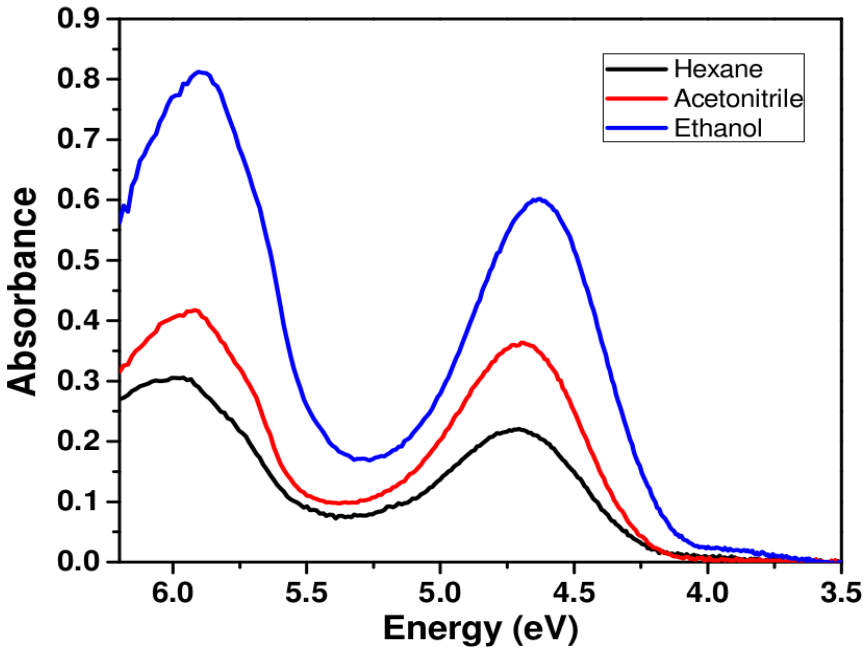

SM11: Experimental absorption spectrum of 3-HOX in different solvents.

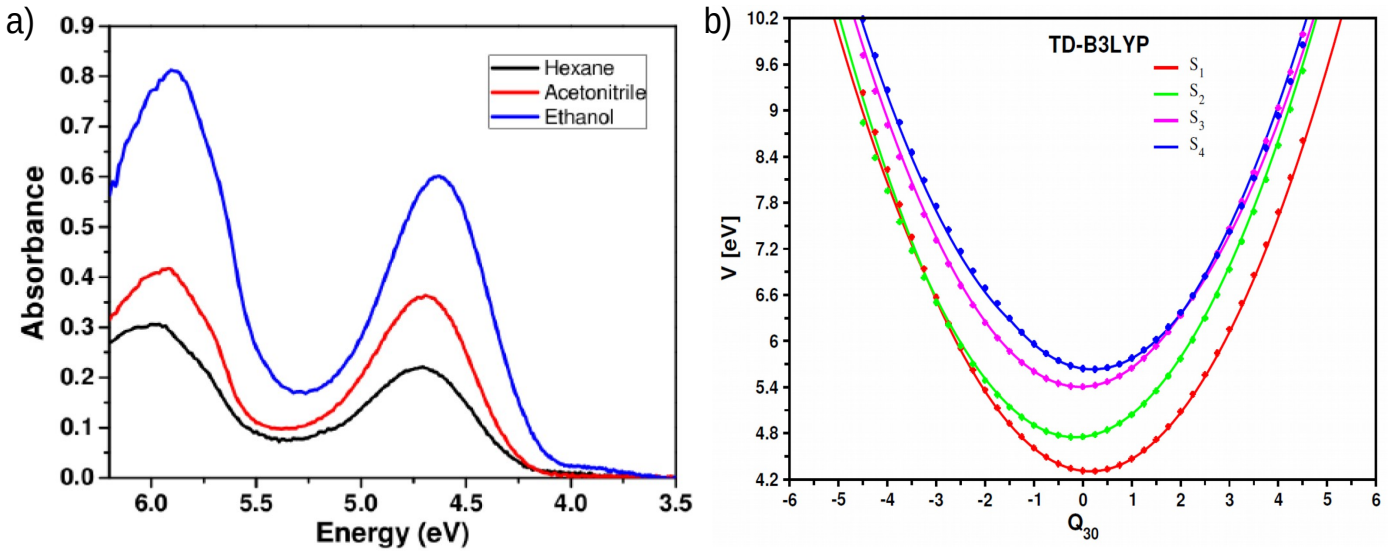

c)

Electronic state	Excitaion energy, in eV (osc. strength)
S_1	4.3113 (0.00)
S_2	4.7554 (0.11)
S_3	5.4053 (0.02)
S_4	5.6421 (0.00)
S_5	5.8654 (0.01)
S_6	6.1249 (0.00)

SM12: a) Experimental absorption spectrum of 3HOX in different solvents. b) Adiabatic potential energy curves of low-lying states along the dimensionless normal coordinates O-H stretch vibration of 3HOX. c) Vertical excitation energy of enol structure with TDB3LYP/6311G++(3df,3pd) level of theory.

Table SM13: Q_c^{min} of totally symmetric vibrations of 3HOX computed within the LVC approach using TDB3LYP/6311G++(3df,3pd) level of theory.

a' mode	Q_c^{min}
ν_3	-0.70
ν_5	1.33
ν_7	0.13
ν_8	0.47
ν_{11}	-0.74
ν_{14}	-0.20
ν_{16}	-1.01
ν_{17}	-0.11
ν_{18}	0.21
ν_{19}	-0.34
ν_{20}	0.21
ν_{21}	0.72
ν_{22}	-0.50
ν_{23}	-0.63
ν_{24}	-0.29
ν_{25}	-0.54
ν_{26}	0.29
ν_{27}	-0.03
ν_{28}	0.06
ν_{29}	0.02
ν_{30}	-0.11

a)

Electronic state (Keto tautomer)	Vertical Excitaion energy, in eV (osc. strength)
S_1	3.4629 (0.08)
S_2	3.6866 (0.00)
S_3	4.8740 (0.05)
S_4	5.0518 (0.00)
S_5	5.1833 (0.00)
S_6	6.5241 (0.00)

b)

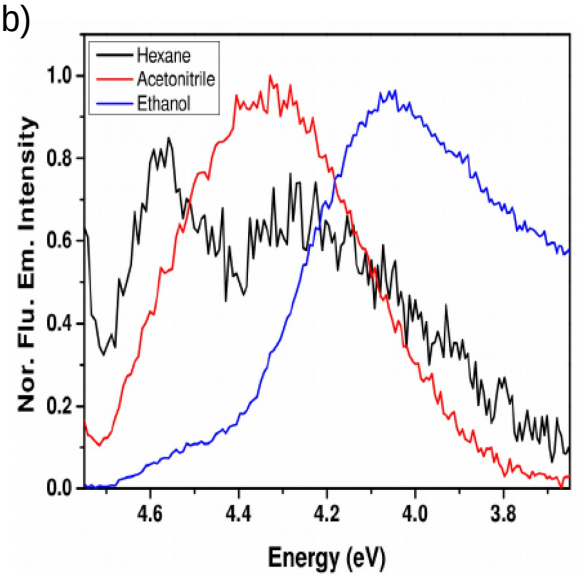

SM14: a) Vertical excitation energies of keto tautomer of 3HOX. b) Experimental fluorescence spectrum of 3HOX in different solvents.

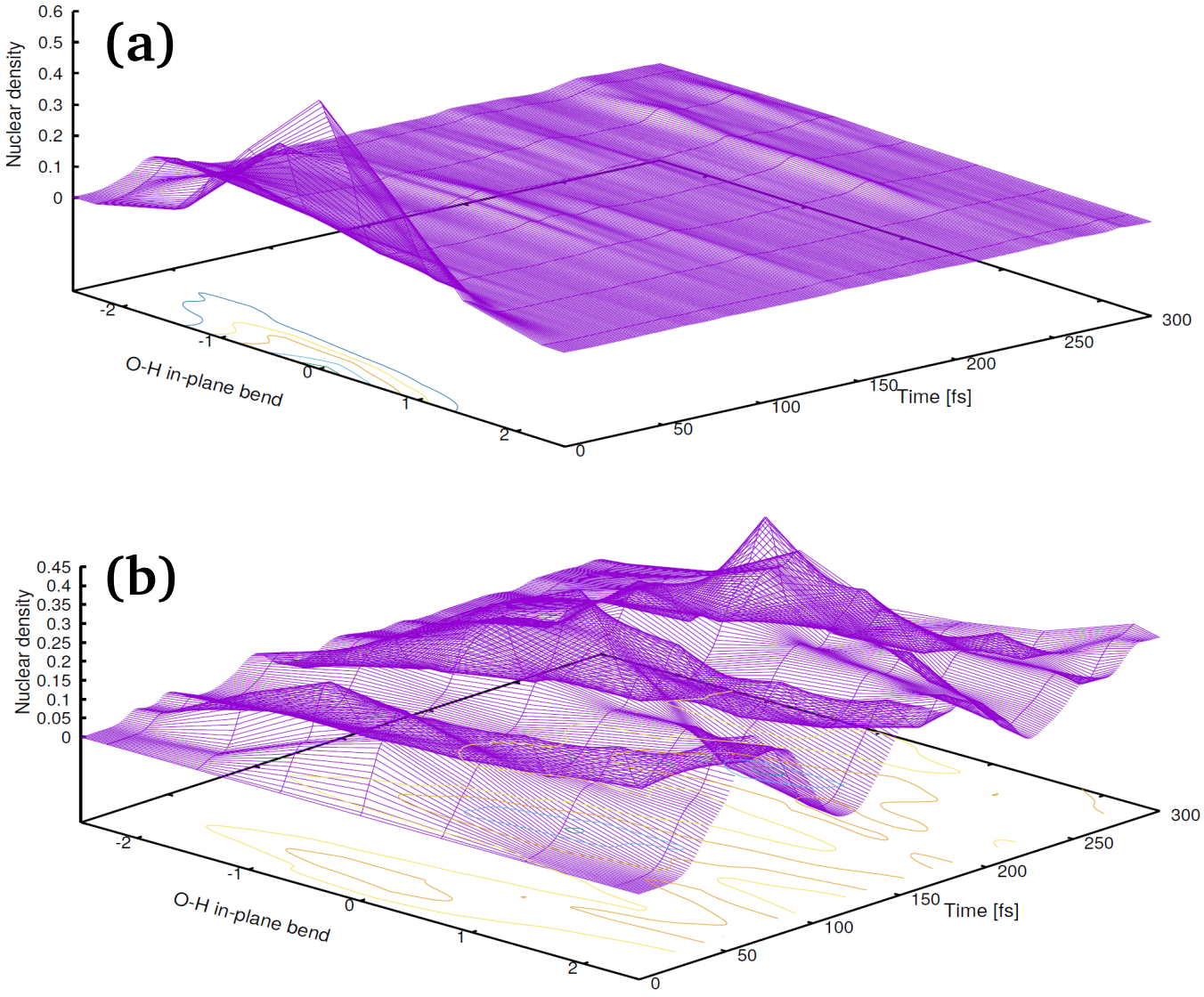

SM15: Time evolution of 1-dimensionl nuclear density along the O-H in-pane bend coordinates (initial wavepacket on S_2 state) for (a) S_2 state (b) S_1 state.

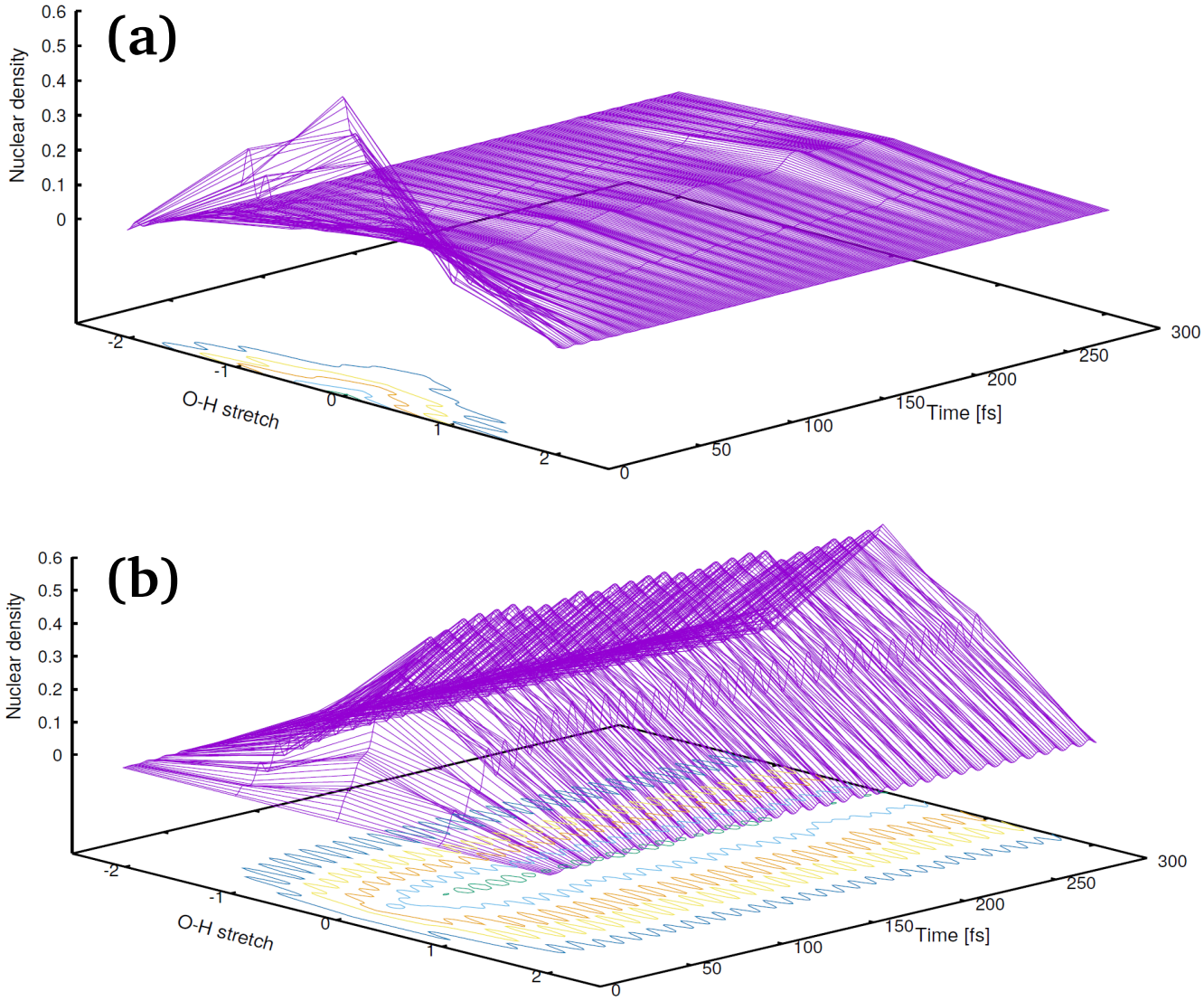

SM16: Time evolution of 1-dimensionl nuclear density along the O-H stretch coordinates (initial wavepacket on S_2 state) for (a) S_2 state (b) S_1 state .

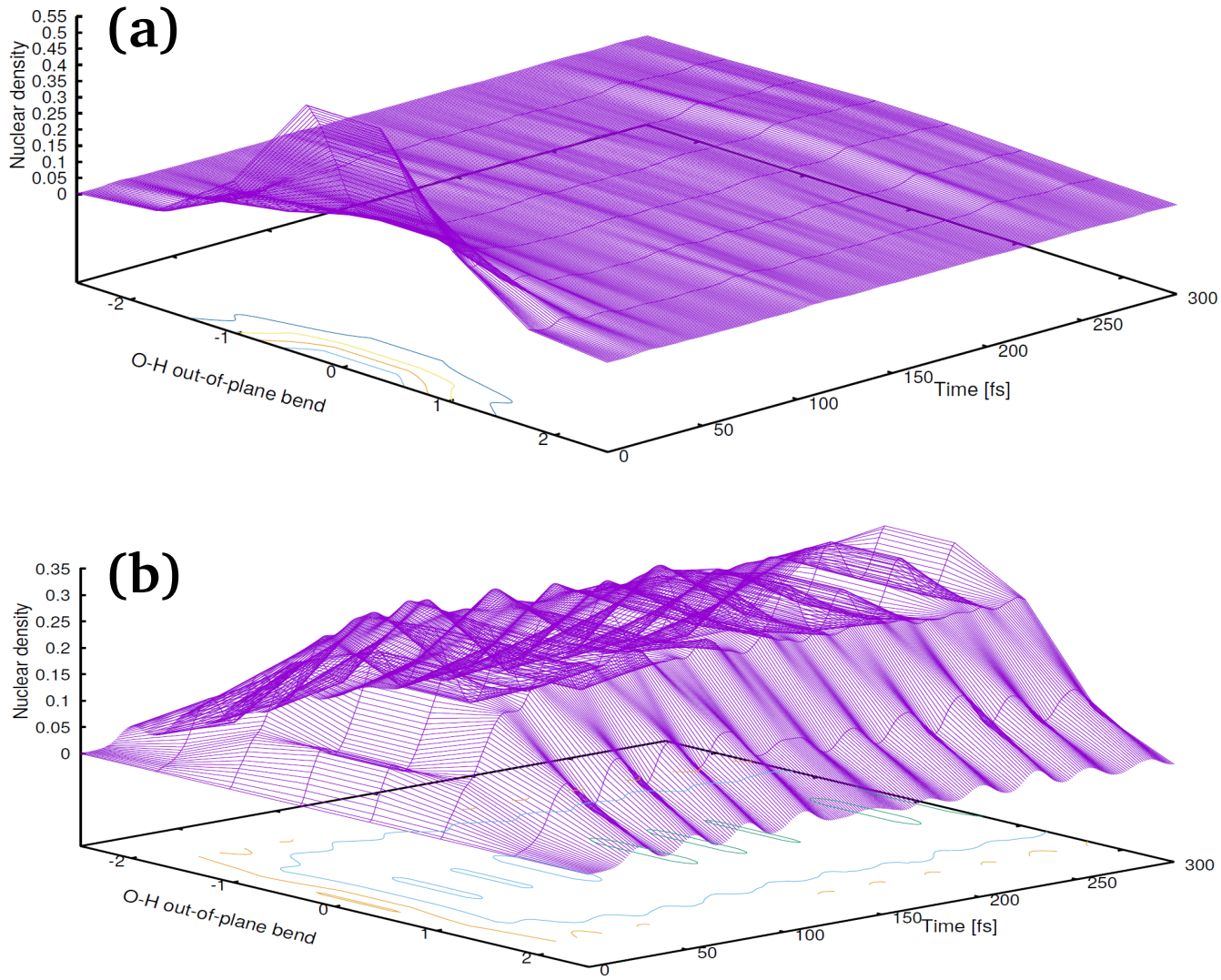

SM17: Time evolution of 1-dimensionl nuclear density along the O-H out-of-plane coordinates (initial wavepacket on S_2 state) for (a) S_2 state (b) S_1 state.